PARSEC-SCALE X-RAY FLOWS FROM O STAR WINDS IN GALACTIC HII REGIONS

Leisa Townsley[1]
Eric Feigelson[1]
Thierry Montmerle[2]
Patrick Broos[1]
You-Hua Chu[3]
Gordon Garmire[1]
Konstantin Getman[1]

[1]*Penn State University, Department of Astronomy & Astrophysics*

[2]*Grenoble Observatory*

[3]*University of Illinois, Department of Astronomy*

Support provided by NASA contract NAS8-38252 to Gordon Garmire, the ACIS Principal Investigator, and by the Chandra X-ray Observatory GO2 grant G01-2008X.

ABSTRACT

We present ACIS images of several high-mass star forming regions, including the Omega Nebula (M 17), the Rosette Nebula (NGC 2237–2246), and the giant HII region complex W 51. The massive clusters powering these HII regions are resolved at the arcsecond level into hundreds of stellar sources, similar to those seen in closer young stellar clusters. However, we also detect diffuse X-ray emission on parsec scales that is spatially and spectrally distinct from the point source population. For the nearby regions (M 17 and Rosette) the emission is soft, with plasma temperatures less than 10 million degrees. This is in contrast to what is seen in more distant complexes (e.g. Arches, NGC 3603).

This extended emission most likely arises from the fast O-star winds thermalized either by wind-wind collisions or by a termination shock against the surrounding media. We establish that only a small portion of the wind energy and mass appears in the observed diffuse X-ray plasma; in the blister HII regions, we suspect that most of it flows without cooling into the low-density interstellar medium through blow-outs or fissures in the surrounding neutral material. These data provide compelling observational evidence that strong wind shocks are present in HII regions.

INTRODUCTION

Massive star-forming regions present a microcosm of starburst astrophysics, where stellar winds from O and Wolf-Rayet stars compete with supernovae to carve up the neutral medium from which they formed and to return processed material to the ISM.

Chandra is revolutionizing star formation studies, finally giving us the sensitivity and spatial resolution to detect diffuse emission and to separate it from the hundreds of X-ray-emitting stars in these fields.

Details in our new paper:
"Ten Million Degree Gas in M17 and the Rosette Nebula: X-ray Flows in Galactic HII Regions," Townsley et al. 2003, ApJ 593, 874

Technology: see poster by Broos et al.

OVERVIEW

- What lurks within the Strömgren Sphere?

- The Rosette Nebula: discovering soft X-rays from OB winds.
- M17, the Omega Nebula: an X-ray champagne flow.
- RCW 49: OB/Wolf-Rayet detente.
- W51: X-rays, X-rays everywhere.

- After all that, where do we stand?

ISM BUBBLES AND HOLLOW HII REGIONS

- UV P Cygni profiles in Orion supergiants discovered by Morton in 1967 (ApJ 150, 535). Can't ignore O star winds anymore!
- Weaver et al. 1977 (ApJ 218, 377) describe an "interstellar bubble" blown by an early-type star with a steady wind into a uniform ambient ISM, filled with 10^{6-7} degree gas. $R > 20$ pc for an O7 star. The usual $T = 10^4$ K HII region starts outside this.
- Dorland, Montmerle, & Doom (1986, A&A 160, 1) and Dorland & Montmerle 1987 (A&A 177, 243) predict smaller region, harder X-rays.
- Dyson and collaborators (1986 - present) consider dense clumps of matter close to massive star, generate "mass-loaded" winds that lead to bubbles center-filled with X-rays.
- UCHIIR's: Strickland & Stevens 1998 (MNRAS 297, 747) predict a hard X-ray component with $L_x \sim 10^{35}$, although most emission should be in far UV.
- Compact clusters of O stars (Cantó, Raga, & Rodríguez 2000, ApJ 536, 896) require wind collision calculations, imply $L_x \sim 10^{35}$ and hard X-rays.

THE ROSETTE NEBULA

- Hollow blister HII region: radio, IR brighter on rim than center.
- D = 1.4 kpc; $10' \sim 4.1$ pc. Age ~ 1.9 Myrs.
- One O4, one O5, 5 late-O stars; all separated by a few parsecs.
- Sits on the edge of the Rosette GMC, containing IR clusters, protostars.
- The ACIS mosaic (4 20-ksec snapshots) steps from the HII region, across the PDR, into the Rosette Molecular Cloud.
- The mosaic reveals ~ 1000 X-ray point sources; we remove them to study the remaining unresolved emission.

Fig. 1.— Rosette Nebula and Rosette Molecular Cloud (RMC): 4 20-ksec ACIS-I snapshots, stepping from the HII region (westernmost pointing) east, across the PDR, and into the RMC to sample IR clusters there. Soft (0.5–2 keV) emission in red, hard (2–8 keV) in blue, smoothed with *csmooth*.

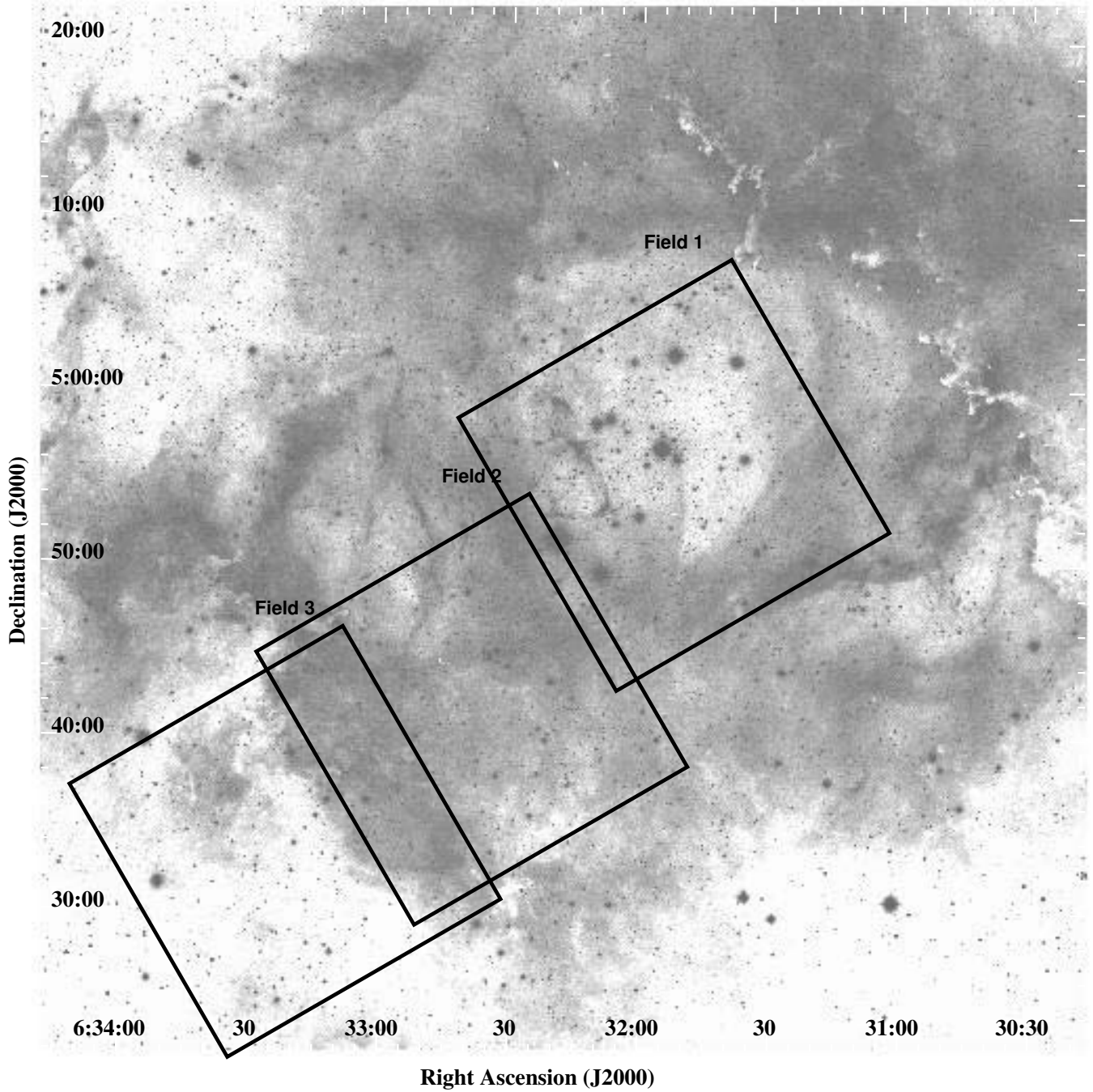

Fig. 2.— A Digitized Sky Survey image of the Rosette Nebula, with three of the four ACIS-I pointings overlaid. This shows the relations between the visual and X-ray emission: diffuse soft X-rays appear to fill the central hole in the Nebula.

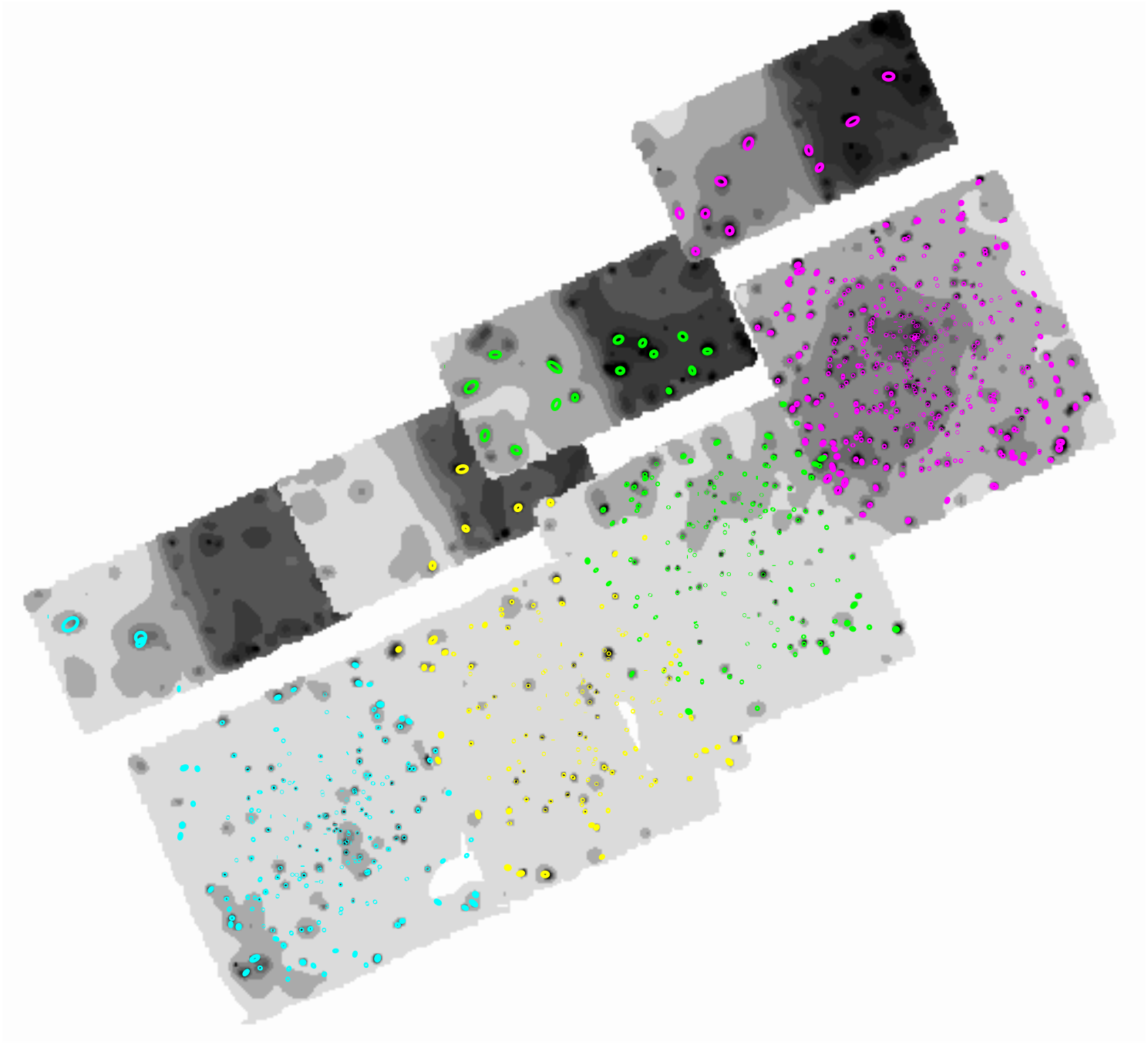

Fig. 3.— The ACIS mosaic of Rosette with $\sim$ 1000 point source extraction regions overlaid. These point sources were removed from the data by extracting counts in regions $\sim$ 1.1 times the PSF size for each source, leaving what we call the "swiss-cheese" dataset for the study of diffuse emission.

ACIS_EXTRACT

See the poster by Broos et al.

New IDL code by Patrick Broos, ACIS_Extract performs automated point source extraction and spectral fitting, generates lightcurves, photometry, diagnostic plots, etc. Latest version will be released end of Sept.

- Multiple observations of a target are handled (weighted ARFs, RMFs).
- Source extraction regions are polygons that follow the Chandra PSF.
- ARFs are lowered by the computed PSF fraction (as a function of energy) to improve flux estimates.
- PSF-correlation and data centroid positions are calculated for each source, can be used to improve source positions.
- Automated spectral fitting is performed using the composite source spectra, background spectra, RMFs, and ARFs.
- Sample XSPEC model scripts are provided.

Konstantin Getman has developed utilities for choosing best spectral fit and for generating LaTeX tables of photometry and fit parameters.

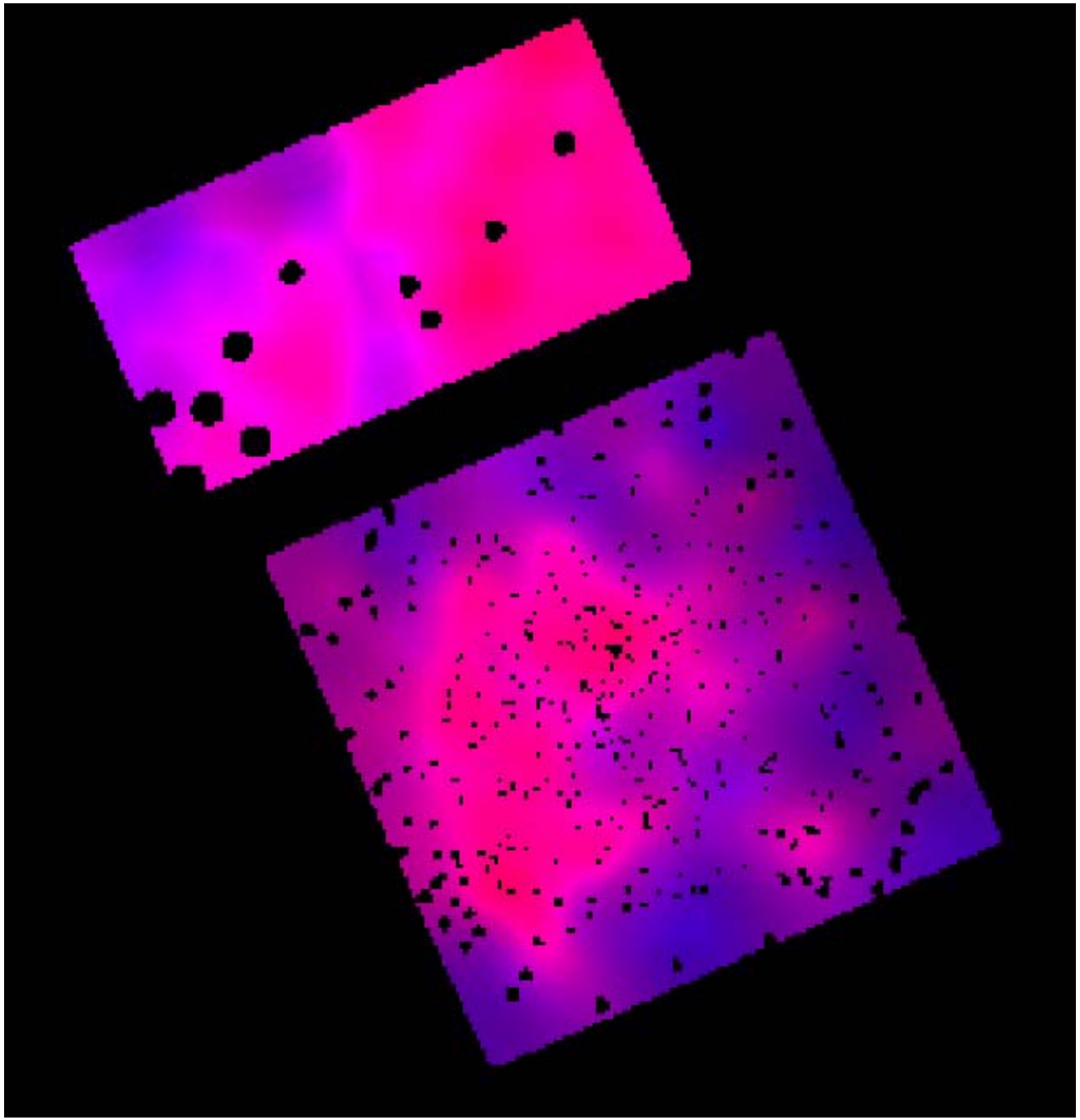

Fig. 4.— Using an adaptive-kernel smoothing technique developed by Patrick Broos, we can highlight the diffuse emission in Rosette by smoothing the swiss-cheese images. This shows the first ACIS pointing centered on the Rosette Nebula, now including all six chips in the ACIS-I array. Diffuse emission may be present in the northern region as well as in the center of the nebula.

M17, THE OMEGA NEBULA

- Bright blown-out blister HII region, strong thermal radio source, high ionization.
- D = 1.6 kpc; $10' \sim 4.7$ pc. Age ~ 1 Myr.
- Edge-on version of Orion K-L region, a blister on the edge of a GMC with an UCHIIR, water masers, and the massive, dense core M17SW.
- 100 stars earlier than B9 (Orion has 8). 14 O stars.
- Several O4/O5 stars form the Ring of Fire, $\sim 1'$ in diameter.

Fig. 5.— $\sim 15' \times 15'$ 2MASS image of M17, centered on the Ring of Fire.

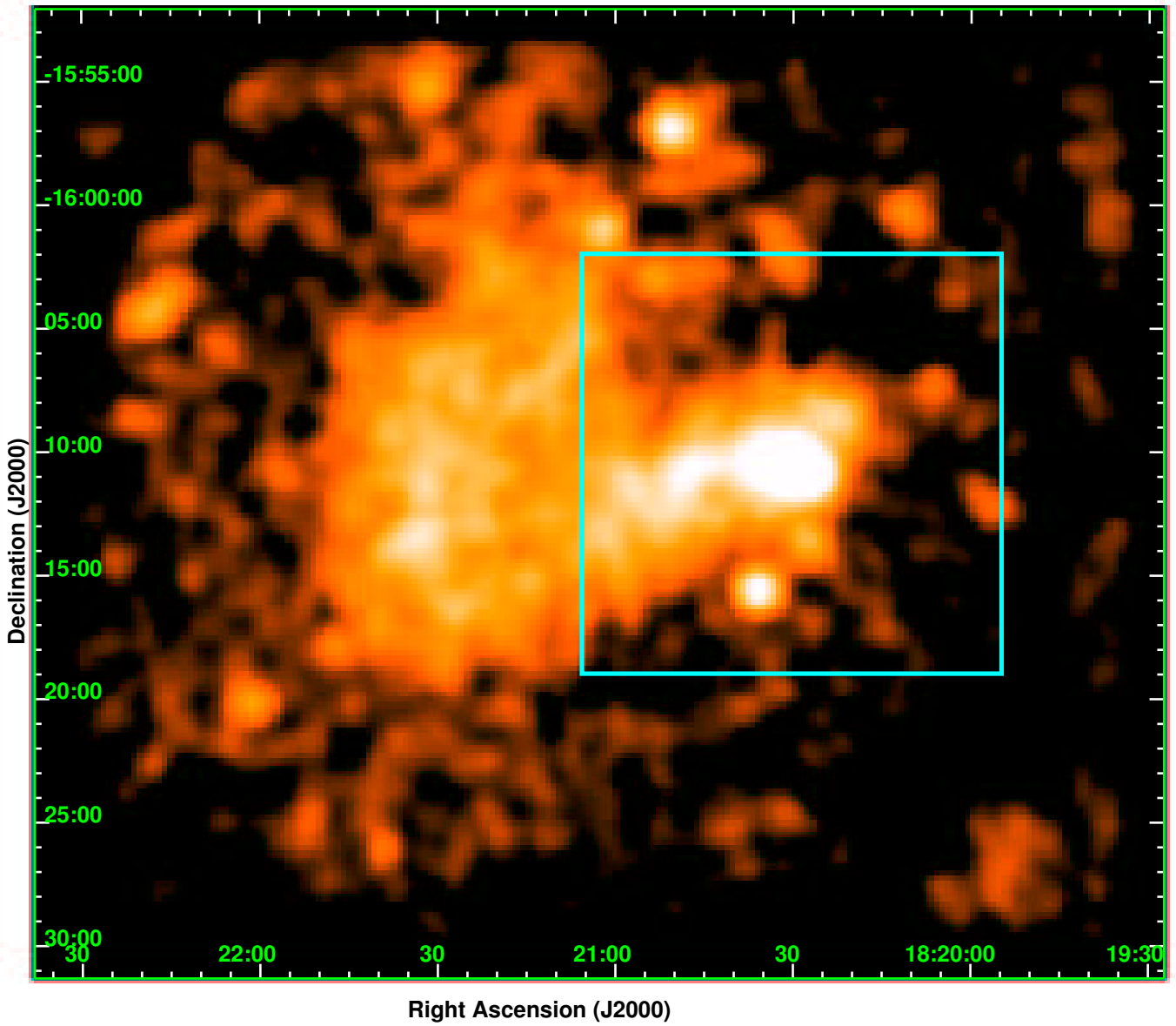

Fig. 6.— Smoothed ROSAT PSPC image of M17, with the outline of the ACIS-I pointing overlaid. For an analysis of the ROSAT data, see Dunne et al. 2003, ApJ 590, 306.

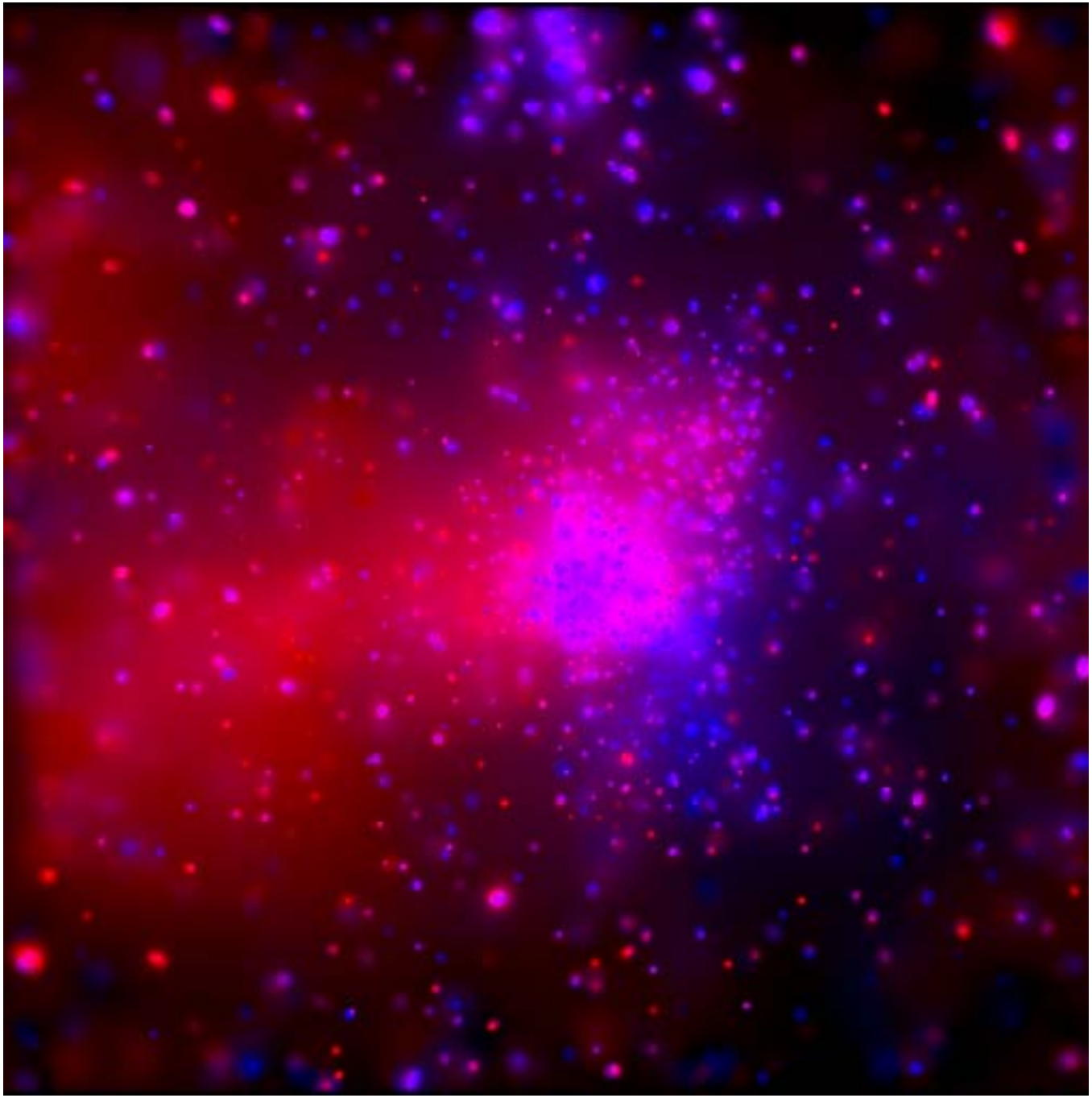

Fig. 7.— The 40-ksec ACIS-I observation of M17, smoothed with *csmooth*. Red intensity is scaled to the soft (0.5–2 keV) emission and blue intensity is scaled to the hard (2–8 keV) emission.

THE M17 POINT SOURCES

See the poster by Getman et al.

A paper on the M17 X-ray point source population is in preparation (Getman et al. 2003).

- $\sim$ 900 ACIS point sources, more than half < 20 counts.
- Simple spectral analysis performed on 348 sources.
- 134 matches to NIR sources from Hanson et al. 1997.
- $\sim$ 100 sources show possible flaring.

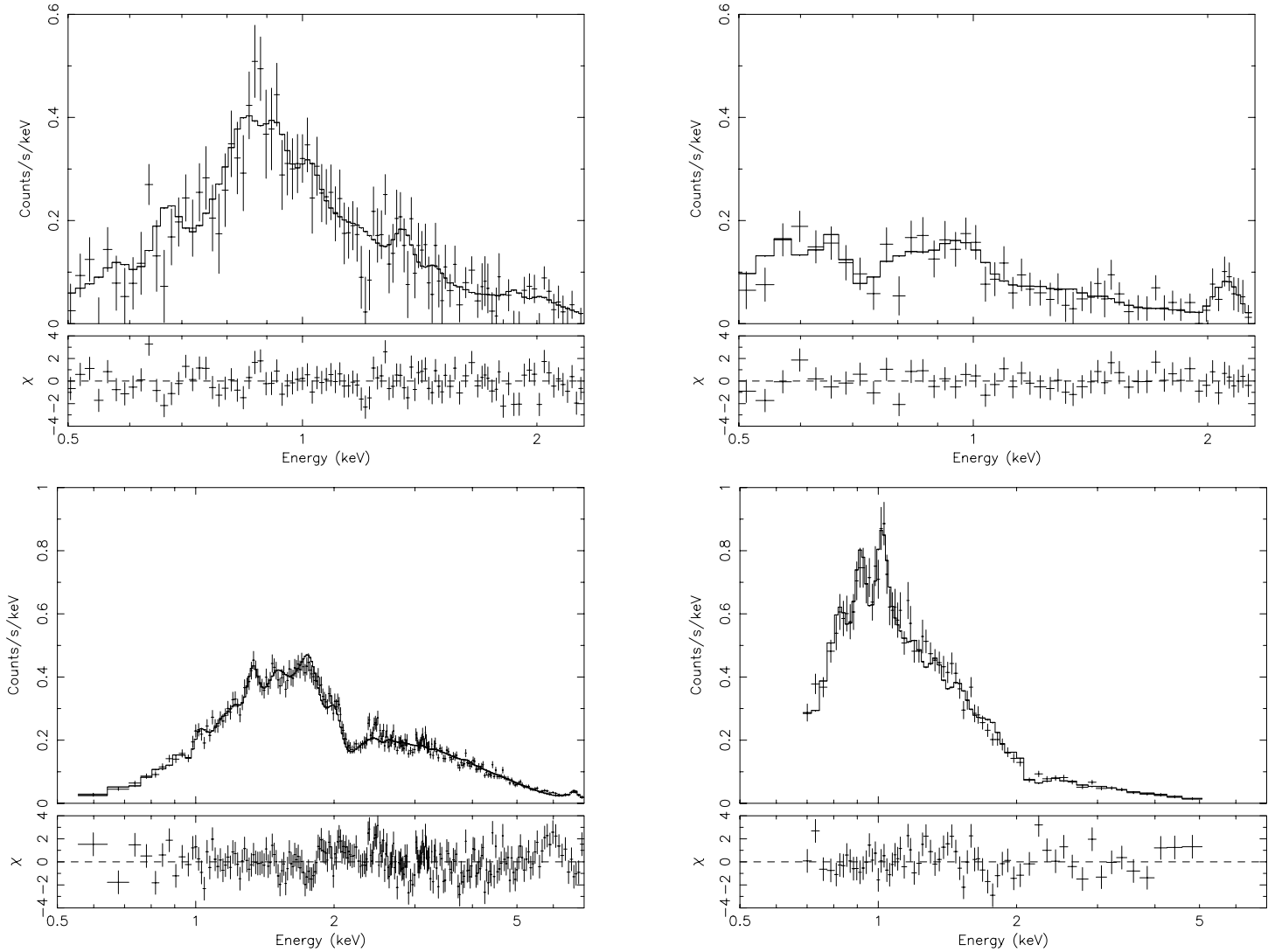

Fig. 8.— ACIS spectra of the following composite components: (Top left) M 17 diffuse emission ($N_H = 4 \times 10^{21}$ cm^{-2}, $kT = 0.13, 0.6$ keV, $L_X = 3.4 \times 10^{33}$ ergs/s); (Top right) Rosette diffuse emission ($N_H = 2 \times 10^{21}$ cm^{-2}, $kT = 0.06, 0.8$ keV, $L_X = 0.6 \times 10^{33}$ ergs/s); (Lower left) M 17 point sources ($kT = 3$ keV); (Lower right) Rosette point sources ($kT = 2$ keV). The upper panels show the data and best-fit models; lower panels give the (Data−Model) residuals. Comparing the diffuse spectra to the composite point source spectra shows that the diffuse emission is not likely to be primarily composed of unresolved point sources.

RCW 49 and Westerlund 2

- Westerlund 2 is the young (2–3 Myr), compact cluster ionizing the massive southern star-forming complex RCW 49.
- Our data support D = 2.3 kpc; $10' \sim 6.7$ pc.
- Morphology dominated by two wind-blown shells, from Westerlund 2 + WR20a and the other from WR20b.
- 6 O7 stars, 2 Wolf-Rayet stars.
- ROSAT found 3 point sources associated with W2, plus diffuse emission.

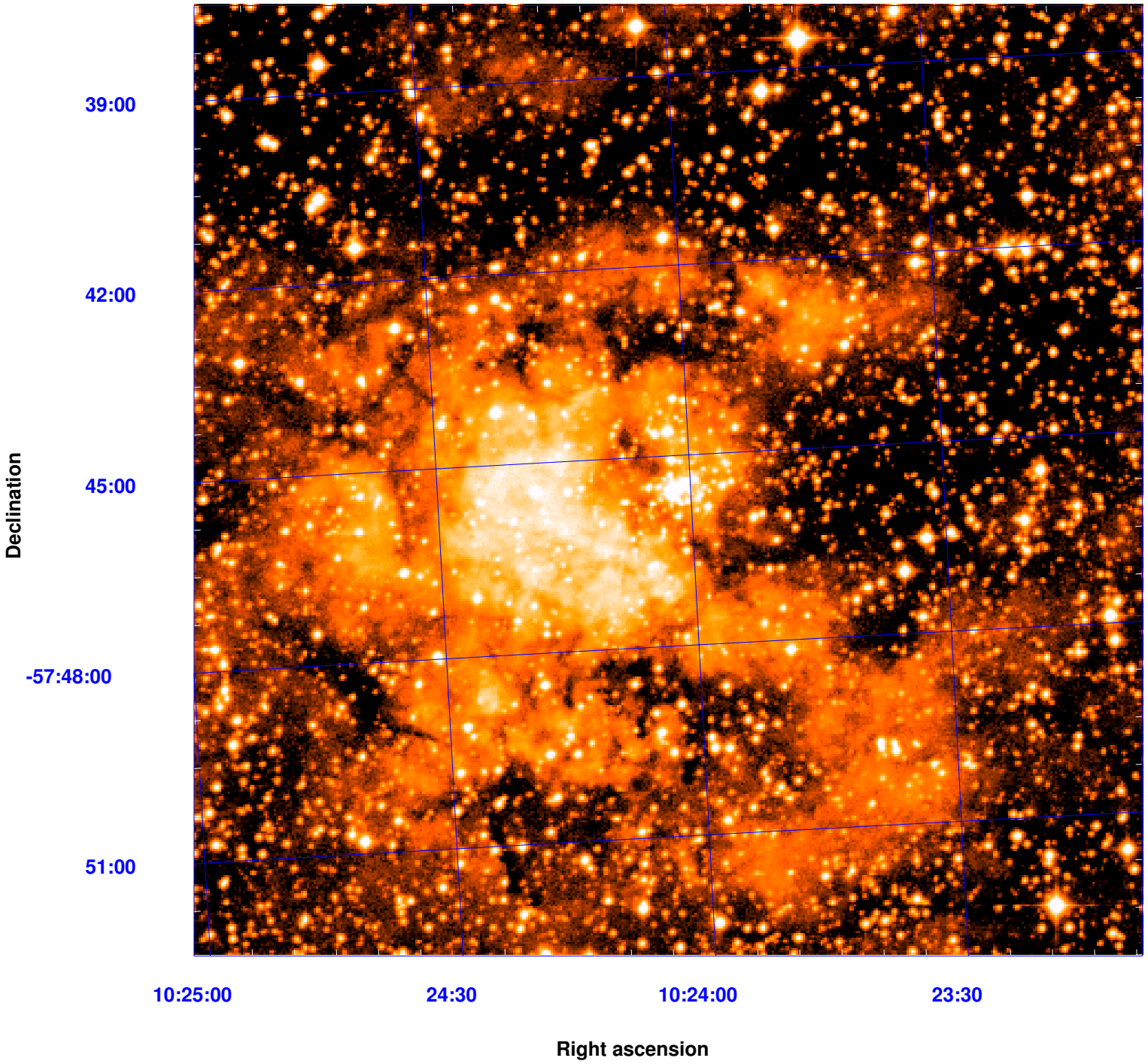

Fig. 9.— POSS2-Red image of RCW 49, approximately the same size as the ACIS-I image.

Fig. 10.— 2MASS image of RCW 49 (Gum 29) centered on its ionizing cluster Westerlund 2, $16' \times 16'$. This cluster and WR20a have created a large wind-blown shell visible in this image; a second shell blown by WR20b is also visible to the southeast.

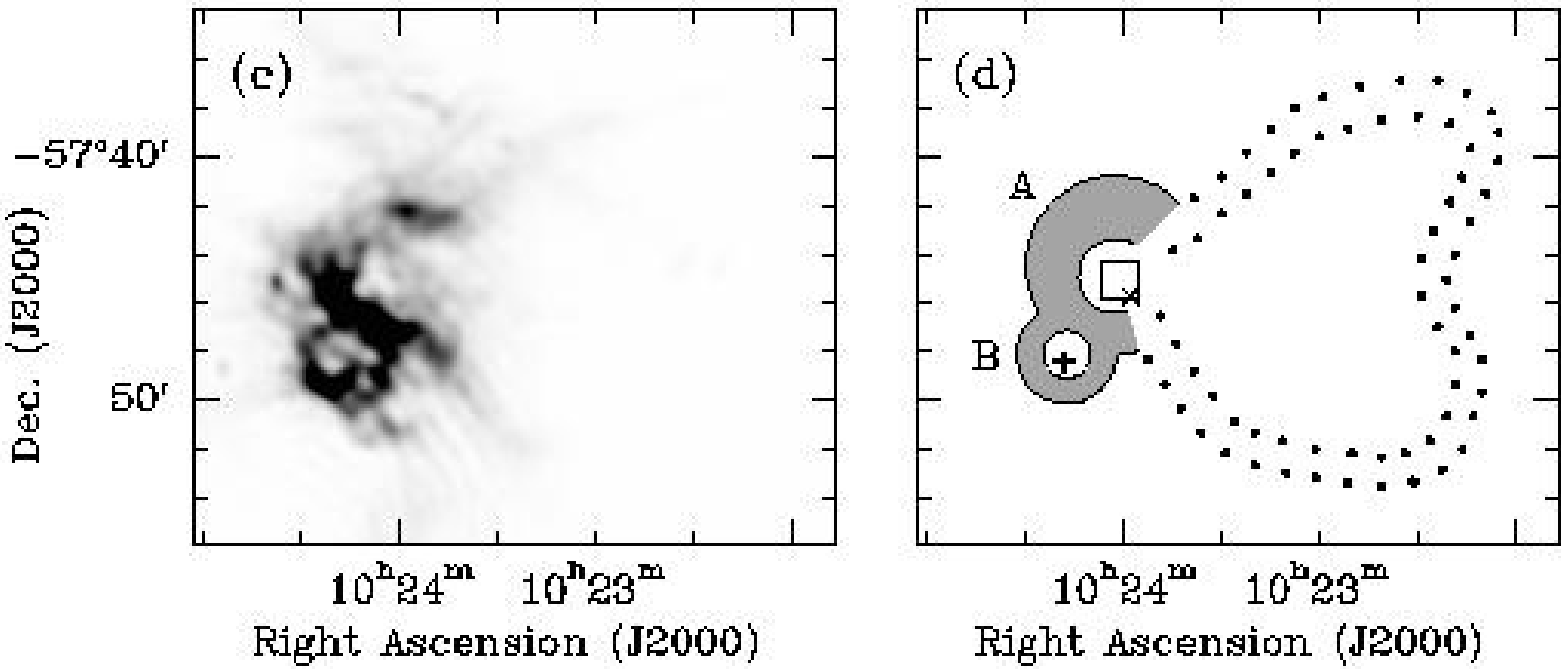

Fig. 11.— A radio image and model of the RCW 49 region, from Whiteoak and Uchida 1997, A&A 317, 563.

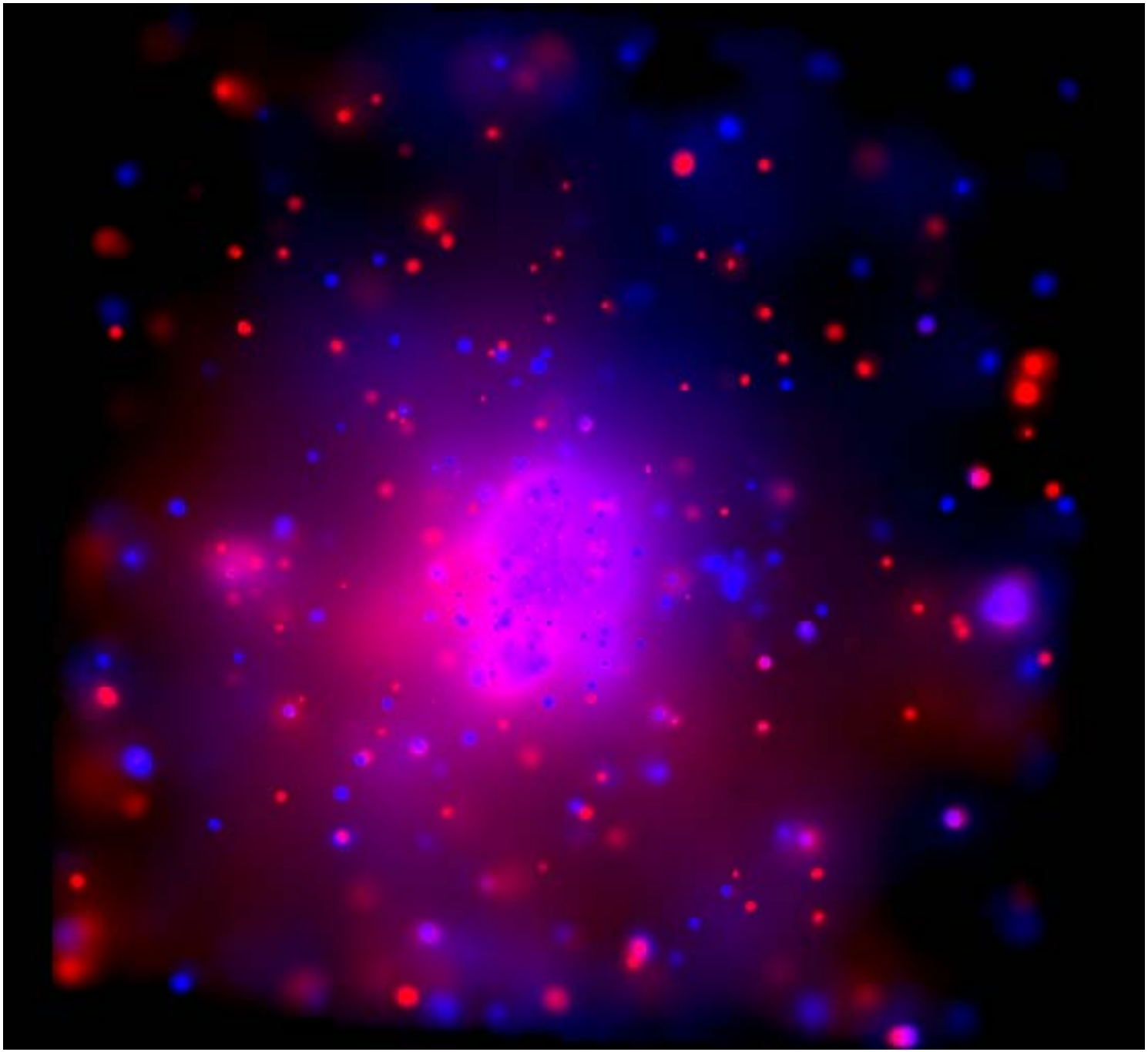

Fig. 12.— The 36-ksec ACIS-I observation of RCW 49, smoothed with *csmooth*. Red intensity is scaled to the soft (0.5–2 keV) emission and blue intensity is scaled to the hard (2–8 keV) emission. Diffuse emission is centered on the ionizing cluster, not obviously associated with the Wolf-Rayet stars.

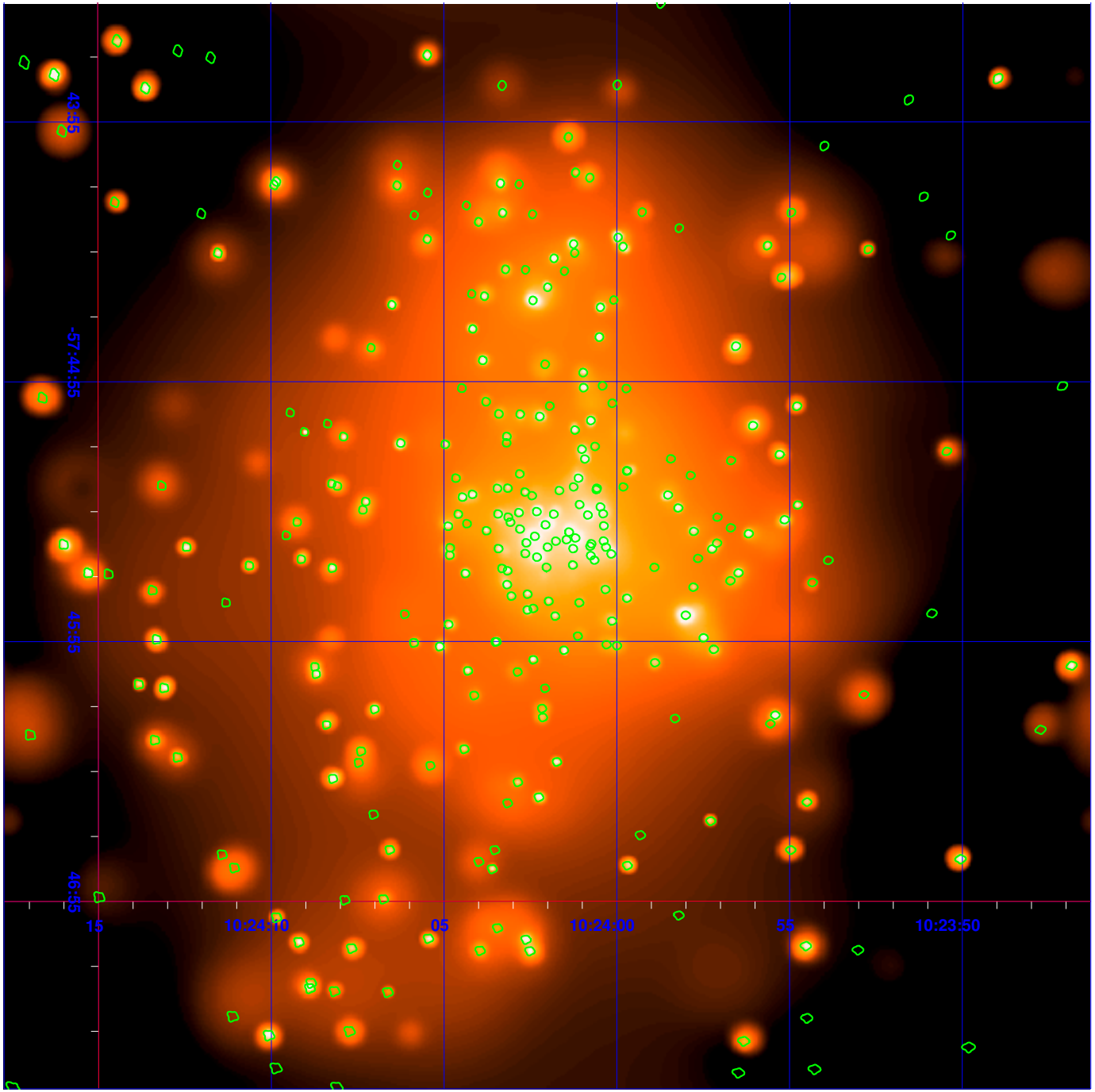

Fig. 13.— The central $\sim 4' \times 4'$ region of the full-band (0.5–8 keV) smoothed ACIS image of RCW 49. Note the large number of resolved point sources and high source density in the central cluster Westerlund 2.

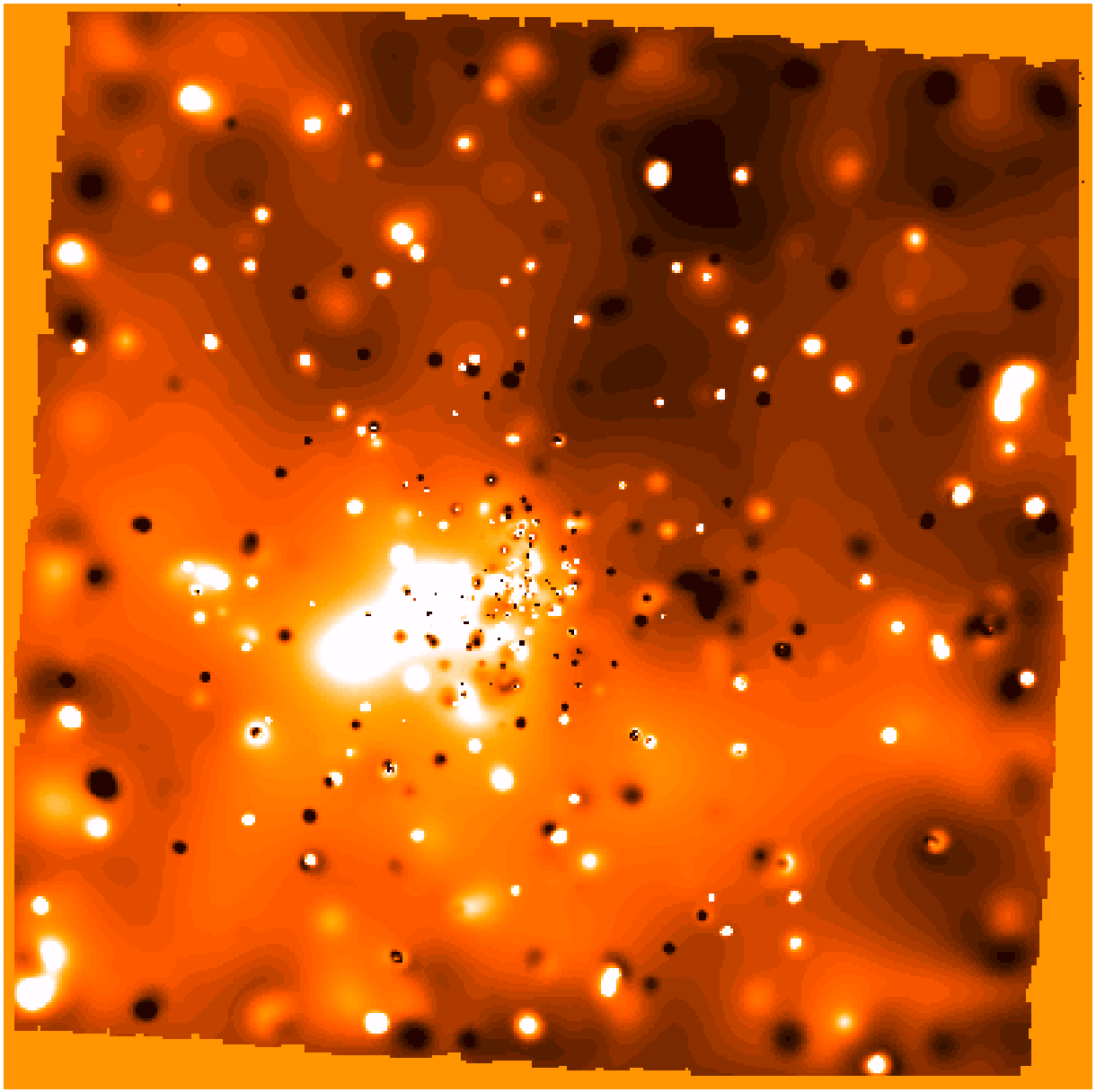

Fig. 14.— A hardness-ratio image of RCW 49: lighter regions are soft, darker regions are hard.

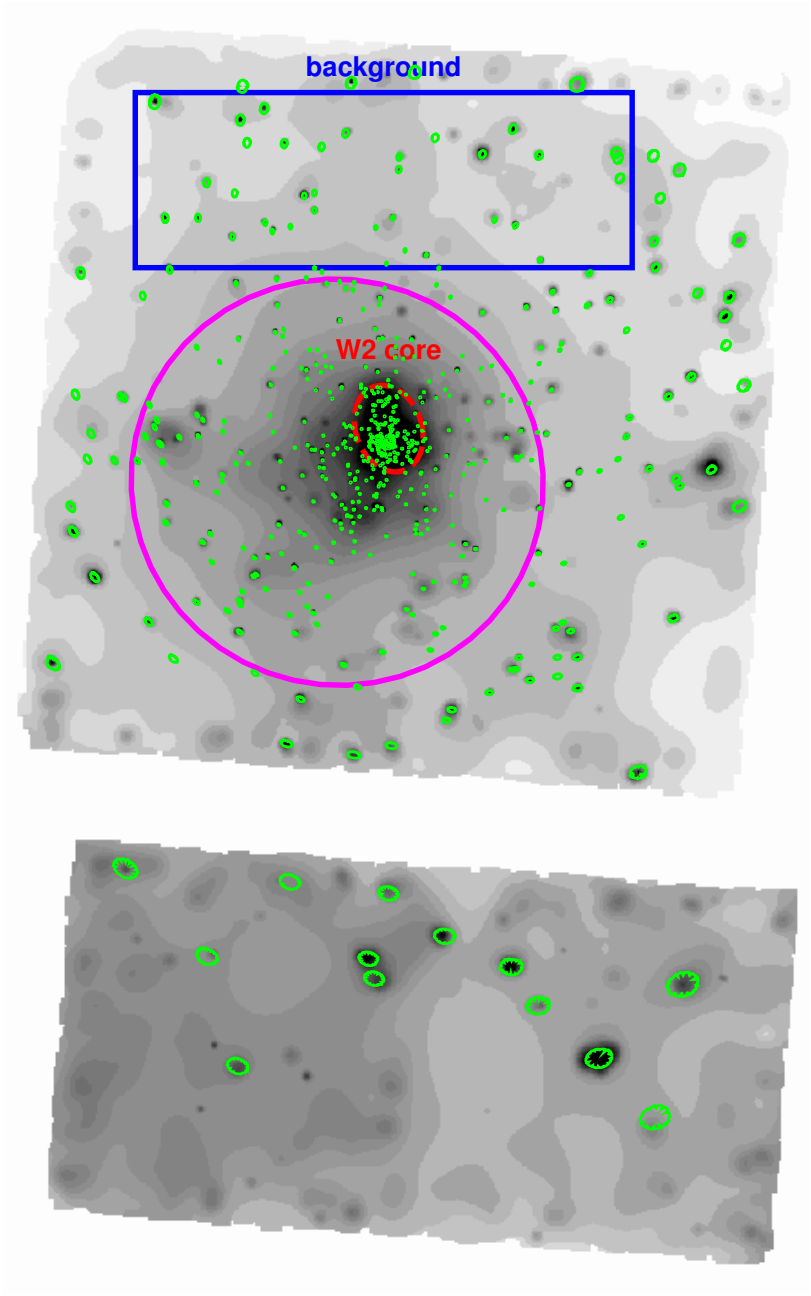

Fig. 15.— A full-band smoothed ACIS image of RCW 49 with over 500 detected point sources outlined in green. The region used to make the diffuse spectrum is the magenta circle (with point source regions and the area outlined in red excluded); the background spectrum was obtained from the blue box. The background almost certainly contains diffuse emission as well as background; we chose to suffer the loss of diffuse photons because the spectral background on the Galactic plane is complex and not well-represented by generic backgrounds taken from other parts of the sky.

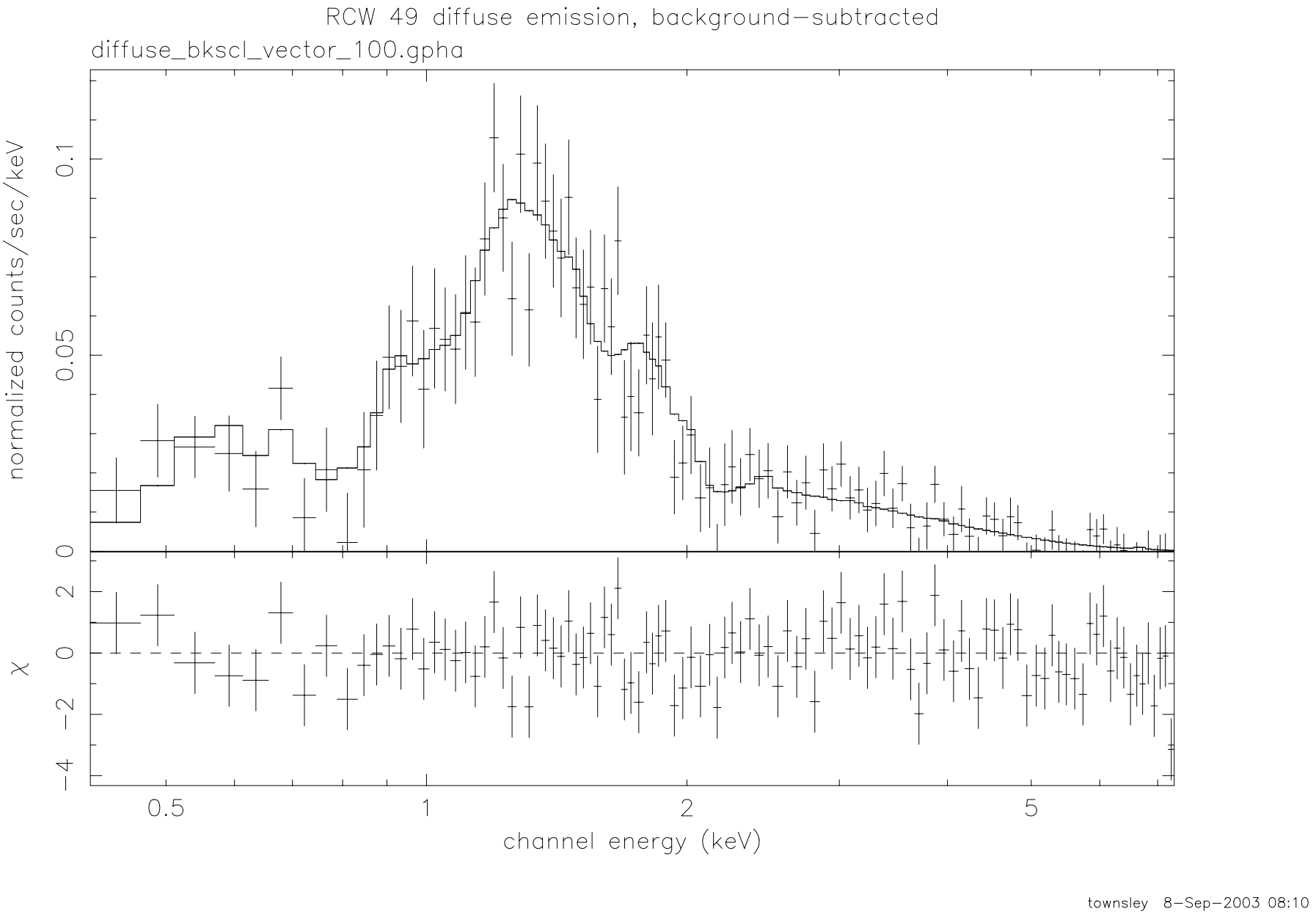

Fig. 16.— A spectral fit to the diffuse emission in RCW 49. Three components are present: a soft thermal plasma ($N_H = 4 \times 10^{21}$ cm^{-2}, $kT = 0.1$ keV); a medium-energy thermal plasma ($N_H = 12 \times 10^{21}$ cm^{-2}, $kT = 0.8$ keV); and a hard component that is not well-constrained by our data ($N_H = 12 \times 10^{21}$ cm^{-2}, both a thermal plasma with $kT \sim 3$ keV or a power law with $\Gamma = 2.3$ give acceptable fits). The X-ray luminosity corrected for absorption is $L_X = 2 \times 10^{33}$ ergs/s.

W51

- One of the most luminous star-forming complexes in the Galaxy; its GMC is in top 10% by mass and top 1% by size.
- D = 7.5 kpc; $10' \sim 21.8$ pc.
- At the tangent point of the Sagittarius Arm, star formation triggered by collisions of huge molecular clouds, perhaps due to spiral density wave.
- Just the complex G49.5-0.4 has 35 O stars (earliest O4); two are supergiants.

Fig. 17.— 2MASS image of the entire W51 complex, $43' \times 71'$; the ACIS pointing covered the massive HII region complex W51A, just above and left of center in this image. Cluster ages range from 0.4 to 2.3 Myr and the complex contains dozens of radio HII regions.

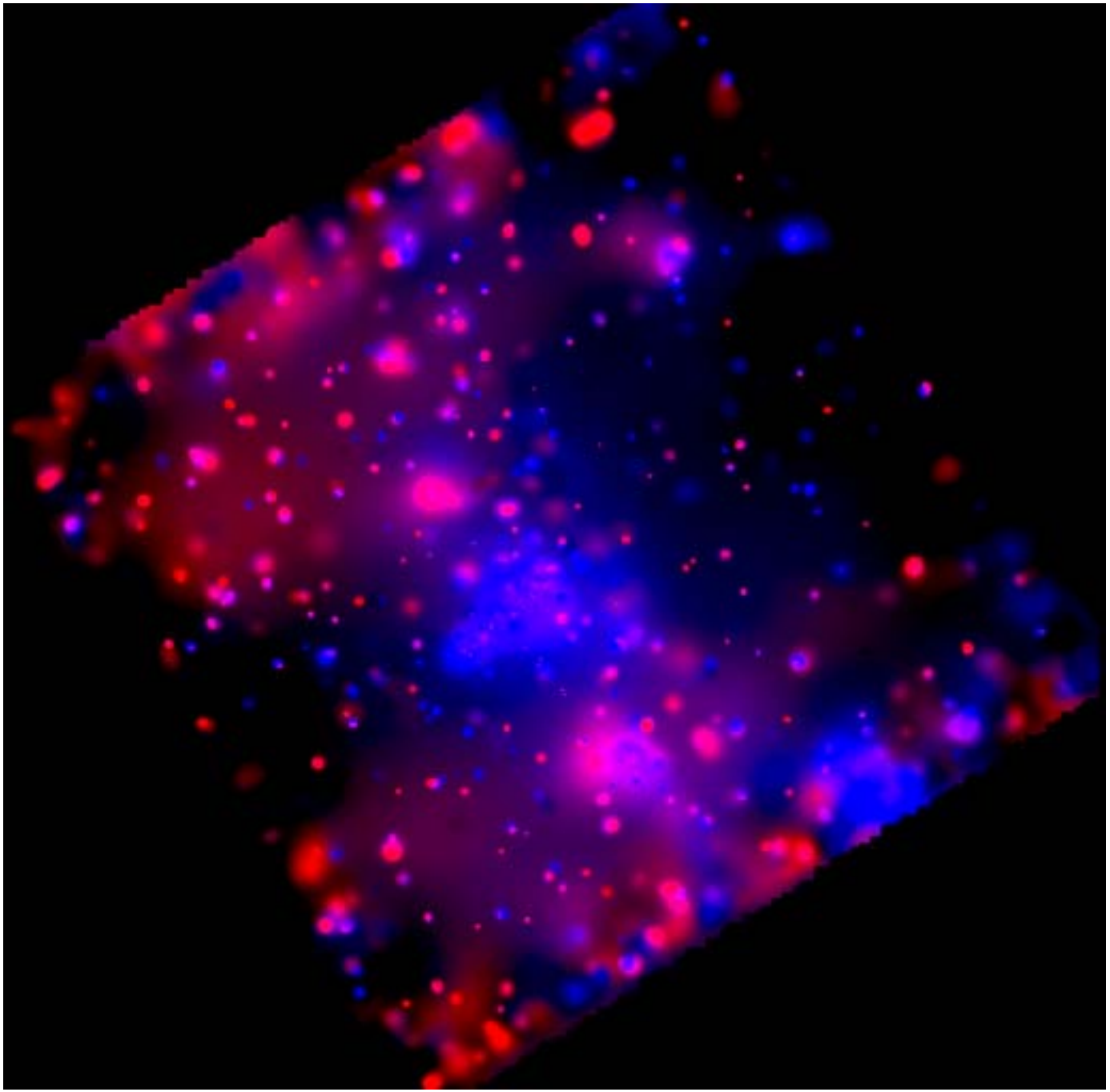

Fig. 18.— The 72-ksec ACIS-I observation of W51A, smoothed with *csmooth*. Red intensity is scaled to the soft (0.5–2 keV) emission and blue intensity is scaled to the hard (2–8 keV) emission. Diffuse emission is associated with many of the known radio HII regions. Over 450 X-ray point sources are detected.

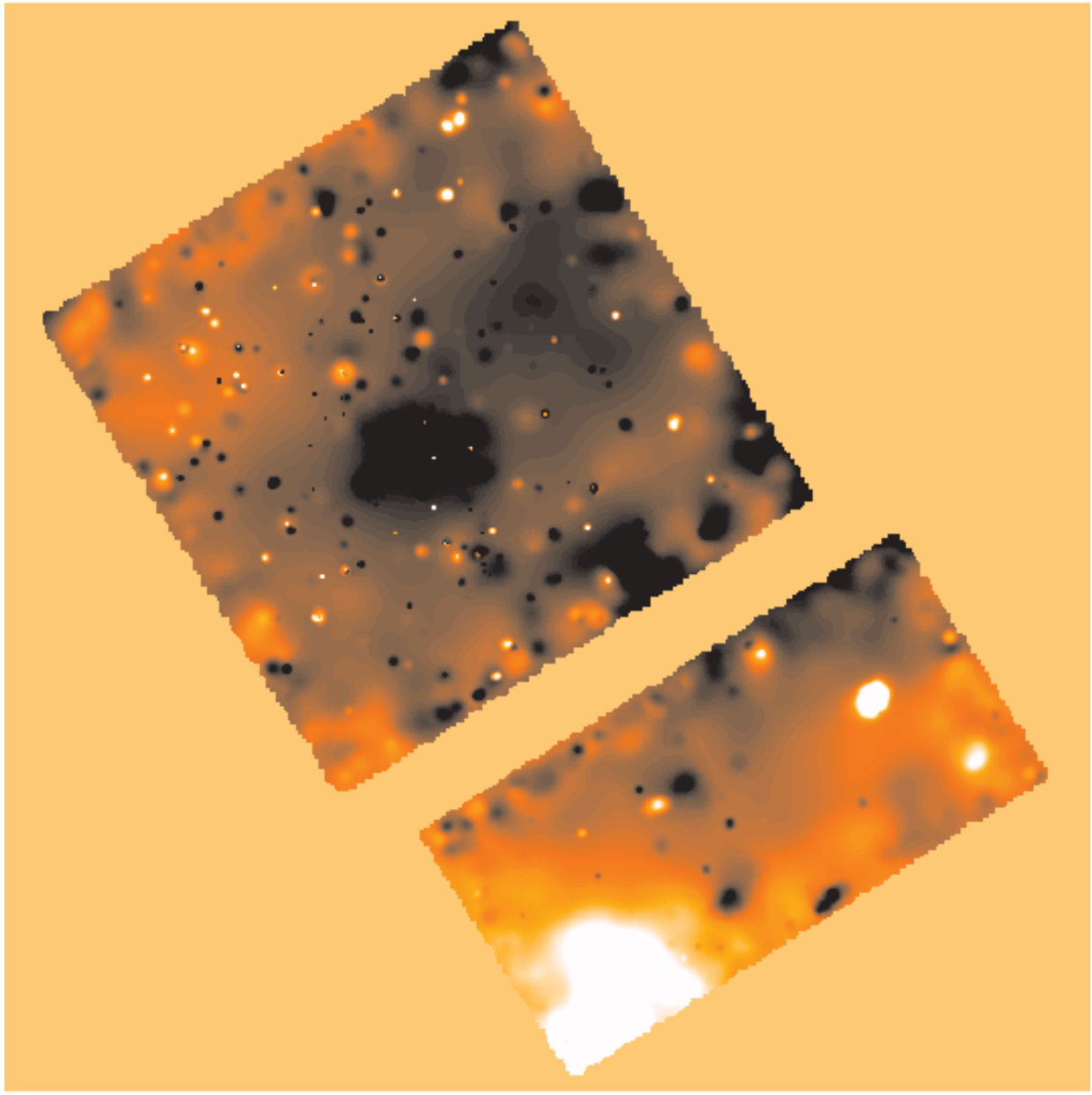

Fig. 19.— A hardness-ratio image of W51A: lighter regions are soft, darker regions are hard. The supernova remnant W51C is seen as a soft extended source at the bottom of the image.

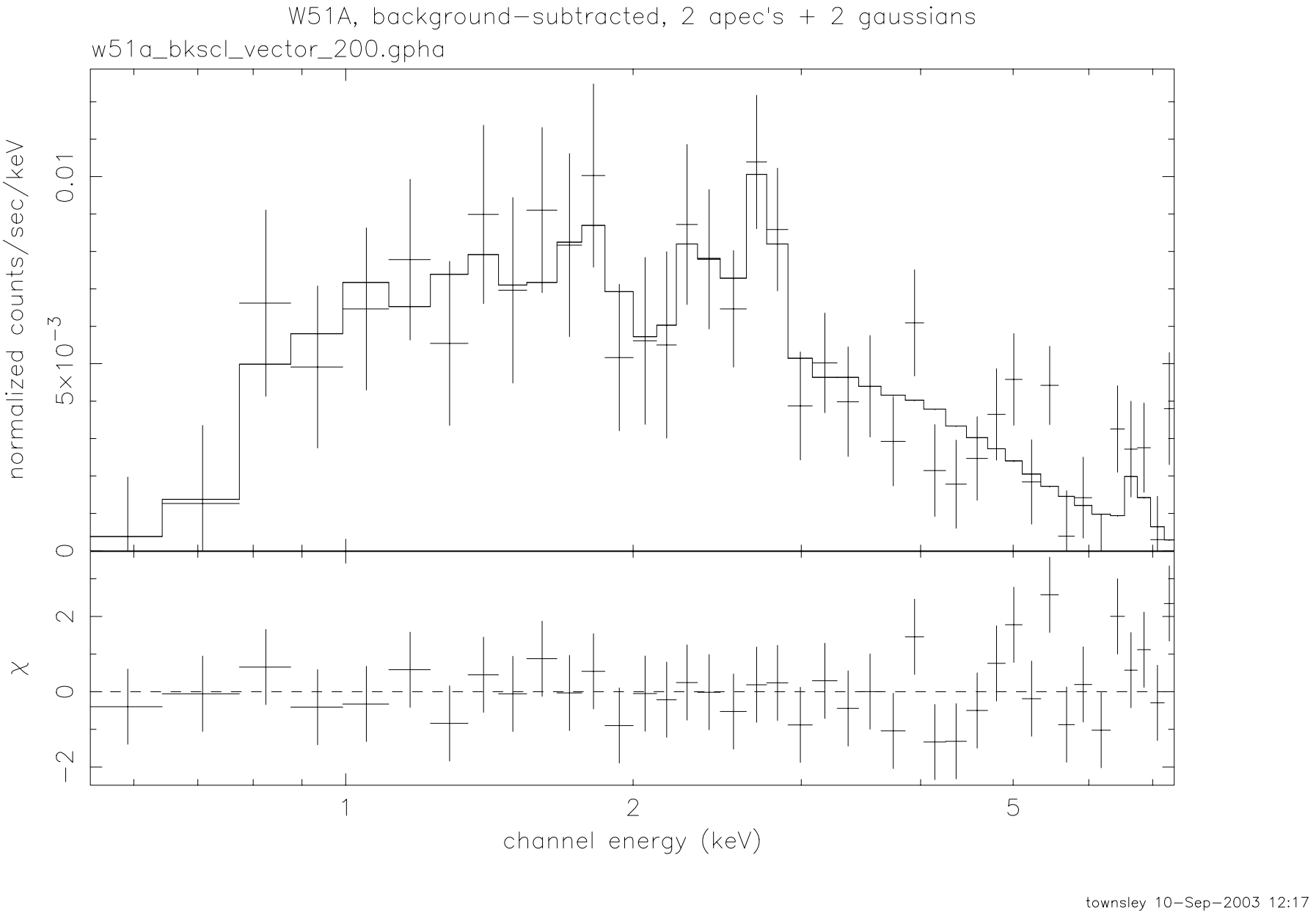

Fig. 20.— A spectral fit to the diffuse emission in G49.5-0.4, the main HII region complex in W51A. Two thermal plasma components plus two gaussians (at 2.3 and 2.7 keV) are necessary to provide an adequate fit: a medium-soft plasma ($N_H = 1 \times 10^{22}$ cm^{-2}, $kT = 0.5$ keV); and a hard plasma ($N_H = 3 \times 10^{22}$ cm^{-2}, $kT = 7$ keV). The X-ray luminosity corrected for absorption is $L_X = 7.6 \times 10^{33}$ ergs/s.

Table 1. Diffuse X-rays from High Mass Star Forming Regions

Region	Diffuse Area (pc^2)	N_H 10^{21} cm^{-2}	kT (keV)	$L_x, corrected$ 10^{33} ergs s^{-1}
Orion Nebula	...	...	...	$< 10^{-3}$
Eagle Nebula	...	...	...	$< 10^{-3}$
Lagoon – NGC 6530	...	...	...	$< 10^{-2}$
Lagoon – Hourglass	0.04	11.1	0.63	≤ 0.7
Rosette Nebula	47	2	0.06, 0.8	≤ 0.6
RCW 38	2	9.5	0.2, $\Gamma = -1.6$	1.6
RCW 49	39	4, 12	0.1, 0.8, 2.8	2
Omega Nebula	42	4	0.13, 0.6	3.4
W51A	140	10, 28	0.5, 7	7.6
Arches Cluster	14	100	5.7	16
NGC 3603	50	7	3.1	20
Carina Nebula	1270	3–40	0.8:	200:

SUMMARY

- *Chandra* has resolved diffuse emission from stellar populations in several Galactic high-mass star-forming regions. *These are the first unambiguous detections of OB "windswept bubbles."*
- The Strömgren Sphere is really a Strömgren Shell in many cases; the X-ray flows we see may significantly affect HII region evolution.
- Diffuse emission not seen in every HII region – seems to require early and/or multiple O stars. Unclear whether emission is from individual stars or wind-wind interactions.
- The theories have to deal with $kT \sim 0.8$ keV and ~ 5 keV (or $\Gamma \sim 2$), $L_x \sim 10^{32-34}$, center-filled morphologies, parsec scales.
- The X-ray luminosities that we report are lower limits to the true emission, due to geometry and obscuration.
- Only a small portion of the wind energy and a tiny fraction of the mass appears in the observed diffuse X-ray plasma. Could be dissipated via turbulence, mass-loading, fissures...
- X-ray flows from HII regions may contribute to galaxian features (Galactic Ridge, diffuse emission in galaxies, starburst superwinds).
- We've just scratched the surface – stay tuned for more data and discoveries!

Already observed:

- NGC 6514 (Trifid)
- M 8 (Lagoon)
- W 3 Main
- Trumpler 16 (eta Carinae)
- M 16 (Eagle)
- NGC 6334 (Bear Claw)
- Cepheus B

Coming in the next year:

- RCW 108
- Arches Cluster
- Cygnus OB2
- Rosette NGC 2244
- NGC 6357 and Pismis 24
- Trumpler 14 in Carina
- XMM Carina mosaic
- NGC 3576 (M 17 analog)